To be presented at the
International Conference on Nuclear Physics,
Munich, Germany, August 27-September 1, 1973

LBL-1968
c.1

ROTATION-ALIGNED COUPLING SCHEME

RECEIVED
LAWRENCE
RADIATION LABORATORY

SEP 11 1973

LIBRARY AND
DOCUMENTS SECTION

F. S. Stephens

July 1973

Prepared for the U. S. Atomic Energy Commission
under Contract W-7405-ENG-48

For Reference

Not to be taken from this room

LAWRENCE BERKELEY LABORATORY
UNIVERSITY OF CALIFORNIA
BERKELEY

LBL-1968
c.1

DISCLAIMER

This document was prepared as an account of work sponsored by the United States Government. While this document is believed to contain correct information, neither the United States Government nor any agency thereof, nor the Regents of the University of California, nor any of their employees, makes any warranty, express or implied, or assumes any legal responsibility for the accuracy, completeness, or usefulness of any information, apparatus, product, or process disclosed, or represents that its use would not infringe privately owned rights. Reference herein to any specific commercial product, process, or service by its trade name, trademark, manufacturer, or otherwise, does not necessarily constitute or imply its endorsement, recommendation, or favoring by the United States Government or any agency thereof, or the Regents of the University of California. The views and opinions of authors expressed herein do not necessarily state or reflect those of the United States Government or any agency thereof or the Regents of the University of California.

0 0 0 0 4 0 0 0 1 2 3

LBL-1968

ROTATION-ALIGNED COUPLING SCHEME*

F. S. Stephens

Lawrence Berkeley Laboratory
University of California
Berkeley, California 94720

*Work performed under the auspices of the U. S. Atomic Energy Commission.

The International Conference on Nuclear Physics, Munich, Germany, August 27 - September 1, 1973.

0 0 0 0 4 0 0 0 4 2 7

1. Introduction

The study of nuclear states with high angular momentum is currently popular. There are probably two essential reasons for this. The first is that the nature of states with spin larger than about 12 $\hbar$ is not yet well understood in any nucleus, and for most nuclei the limits of understanding are at much lower spin values. The second reason is that the heavy-ion compound-nucleus reactions (HI,xnγ) provide a relatively easy and systematic means of populating very high spin states. There are now many laboratories employing heavy-ion accelerators in such studies, and the resulting data pose a number of intriguing questions.

A consideration of some of these questions suggests that a new coupling scheme is often important for very high-spin states. In this scheme the particle angular momentum, j, is quantized along the rotation axis of the nucleus, and hence the name: rotation aligned. This is analogous to the name, deformation aligned, for the usual strong coupling scheme where j is quantized along the deformation (or symmetry) axis. The objective of the present paper will be to define this coupling scheme and to show why and where it is applicable in both the odd-A and even-even nuclei.

2. Rotation-Aligned Coupling Scheme

An over-simplified sketch illustrating the difference between the usual deformation-aligned coupling scheme and the new rotation-aligned scheme is shown in fig. 1. At the top, the deformation-aligned coupling scheme is indicated, where j has a sharp projection, Ω, on the symmetry ($\hat{3}$) axis of the nucleus. The core rotational angular momentum, R, and α, the projection of j on the rotation axis (located somewhere in the $\hat{1},\hat{2}$ plane), are not sharp, as indicated by the multiple-pronged arrows. The wave function for this scheme is the usual one proposed by Bohr[1]), consisting of an intrinsic part, χ^j_Ω , and the rotational D-function. At the bottom of fig. 1, the rotation-aligned coupling scheme is indicated, where α is sharp and R and Ω are not. The wave function here can be written as a linear combination of the deformation aligned ones, where the expansion coefficients are given by the $d^j_{\alpha\Omega}(\pi/2)$ values[2]). There is a third coupling scheme, not shown in fig. 1, where R is sharp and α and Ω are not; this is a variety of the familiar weak-coupling scheme[1,3]). In order to show the conditions under which a particular one of these coupling schemes should be applicable, it is necessary to discuss briefly the particle-plus-rotor model.

The particle-plus-rotor Hamiltonian can be written:

$$H = H_p + H_{rot} = H_p + \frac{\hbar^2}{2\mathcal{J}} \vec{R}^2 = H_p + A\,\vec{R}^2 \quad , \tag{1}$$

where H_p is the particle Hamiltonian in the absence of rotation and $\mathcal{J}$ is the core moment of inertia. The total angular momentum of the system $\vec{I}$ is composed of the core rotational angular momentum $\vec{R}$ plus the particle angular momentum $\vec{j}$, which gives the relation:

$$\vec{R} = \vec{I} - \vec{j} \quad . \tag{2}$$

For the unique-parity, high-j orbitals in each shell it is a very good approximation to consider j to be sharp. Also, the core is assumed to be axially symmetric, so that $R_3 = 0$, and $I_3 = j_3 \equiv \Omega$. Putting eq. (2) into H_{rot} from eq. (1) then gives:

$$H_{rot} = A[I(I + 1) + j(j + 1) - 2\Omega^2] + H_c \quad , \tag{3}$$

where:

$$H_c = -2A[I_1 j_1 + I_2 j_2] = -A[I_+ j_- + I_- j_+] \quad . \tag{4}$$

Under the conditions that j is a good quantum number and that the single-particle Hamiltonian is associated with a quadrupole field oriented along the symmetry axis (the usual Nilsson[4]) potential), H_p can be written:

$$H_p = e_j' + k\beta \left[\frac{3\Omega^2 - j(j + 1)}{4j(j + 1)}\right] = e_j + C\Omega^2 \quad . \tag{5}$$

The coefficient, C, determines how widely the Ω-components of the j-shell are split apart on the Nilsson diagram, and its relationship to the rotational constant, A, determines much of what happens at the lower spin values. It can be shown that eq. (5) is in good agreement with the exact Nilsson solutions for the unique-parity orbitals when $|\beta| \lesssim 0.3$. Substitution of eqs. (3) and (5) into (1) gives:

$$H = e_j + A[I(I + 1) + j(j + 1)] + (C - 2A)\Omega^2 + H_c \quad . \tag{6}$$

For a given situation (I, j and β) the first two terms of eq. (6) are diagonal and the solution of the particle-plus-rotor model consists of diagonalizing the last two terms. When β is large, C is large and A is small, so that H_c is small.

If H_c is negligible, then the solutions are eigenfunctions of the Ω^2 term, which are clearly states with sharp Ω values, and the deformation-aligned (strong) coupling scheme is applicable. However, C and A are not functions of I, whereas H_c increases with I; so that, for large enough I values the opposite situation must occur. That is, at sufficiently large I, the Ω^2 term will be negligible compared with H_c, and the solutions will be eigenfunctions of H_c. It has been shown[2]) that the rotation-aligned wave functions (lower part of fig. 1) are the approximate eigenfunctions of H_c. Thus, for large I values the rotation-aligned coupling scheme should be generally valid. When β is very small, eq. (5) shows that H_p is nearly constant. It can be seen directly from eq. (1) that when H_p is nearly constant (diagonal), the weak coupling scheme with sharp R values will apply. The present case corresponds to a quadrupole-quadrupole particle-core interaction and core states with the rotor energies. These general regions of applicability of the three coupling schemes are clear and rather well known.

However, the rotation-aligned region is extended even to low-spin states when (C - 2A), the coefficient of Ω^2, approaches zero due to the cancellation of the two terms. Since A is always positive, this occurs when C is positive; that is, for prolate deformations in the one-particle H_p given in eq. (5). For a one-hole H_p, the sign of k in eq. (5) is reversed and cancellation occurs for oblate deformations. A convenient way to remember this requirement is to note that the cancellation occurs when the Fermi surface is near the low-Ω orbitals of the j-shell. If reasonable numerical estimates are made for C and A around mass 130 with j = 11/2, then the region where C = 2A occurs for $\beta \approx 0.18$. However, for a considerable region ($\Delta\beta \sim \pm 0.05$) on either side of this value,

(C - 2A) is small and the rotation-aligned scheme is approximately applicable. Many "vibrational" nuclei lie in this region, and much of the interest in this coupling scheme stems from the fact that some regularities in the observed levels of nuclei in this region of β correspond to those expected from the rotation-aligned scheme.

The exact solutions of the particle-plus-rotor model can be obtained by diagonalizing eq. (6) and are shown in fig. 2 for the yrast states coming from the $h_{11/2}$ orbital. At each β value the lowest $I = j$ state is taken to have $E = 0$, and all energies are in units of the corresponding even-even first-excited state energy (E_{2+}). The details of the calculation for this figure have been discussed elsewhere[5]), and only a brief summary will be given here. The Fermi surface was always well below the entire $h_{11/2}$ orbital, so this is a true one-particle case. Pairing was included in the BCS approximation, and a well-established empirical relationship was used to relate A to β. The calculation is for the mass 130 region.

The three coupling-scheme regions discussed above can be readily identified. The nearly degenerate multiplets near $\beta = 0$ are clearly those of the weak-coupling scheme, where one expects such multiplets centered on the core energies. The range where they can be identified is approximately $-0.1 \leqslant \beta \leqslant 0.1$; however, this corresponds roughly to $E_{2+} \geqslant 1$ MeV, and in such cases it is doubtful that any collective model should apply. Thus, in the present context, it is not clear that this coupling scheme will be valid anywhere. The deformation-aligned coupling scheme is valid for large β values and is characterized by normal rotational bands. On the oblate side of fig. 2, the $\Omega = 11/2$ rotational band is recognizable when β is only ~ -0.1, and is rather well developed by $\beta = -0.15$. On the prolate side the anomalous $\Omega = 1/2$ band develops quite slowly, and is not

yet very pure even at $\beta = 0.3$. It has been shown[2]) that the rotation-aligned scheme gives energies virtually identical to these solutions for $0.15 \leqslant \beta \leqslant 0.2$, and is a reasonable approximation for $0.1 \leqslant \beta \leqslant 0.25$. An outstanding regularity of this coupling scheme is the occurrence of the decoupled band[6]) which has: 1) $\alpha = j$ (fully aligned with the rotation axis); 2) spins j, $j + 2$, $j + 4$, ...; and 3) the core energy spacings (as indicated by the adjacent even-even nuclei). The darkened lines in fig. 2 are these states, and this band is seen to persist across the whole prolate side with very nearly the core energy spacings (identifiable at $\beta = 0$). The weak coupling scheme gives the same energies for this band, but requires in addition that other states, $|R - j| \leqslant I \leqslant R + j$, coincide with them. Note that fig. 2 is correct for one (or a few) particles in the $h_{11/2}$ orbital; whereas, for one (or a few) holes the particle-plus-rotor model would give exactly the same results except that the sign of β would be reversed.

The levels that would be populated following a (HI,xnγ) reaction can be predicted rather unambiguously from fig. 2. These would be the lowest-lying high-spin states. On the prolate side this is the decoupled band, and one expects to see stretched E2 transitions and even-even core spacings. The unfavored high-spin states ($j + 1$, $j + 3$, ...) lie considerably higher in energy and will be more weakly populated, if at all. For oblate deformation a normal rotational band (j, $j + 1$, $j + 2$, ...) develops at quite low deformations, and a series of M1 + E2 cascade transitions with E2 cross-overs should be seen. At very low deformations ($\beta \sim 0.1$) the favored and unfavored yrast states lie close together, but the order of favored lowest on the prolate side and unfavored lowest on the oblate side is always preserved. For hole states (nearly full j-shell), all these predictions should occur for the opposite sign of β. It is now of interest to look at some odd-mass nuclei to see if these features occur as expected.

3. Odd-Mass Nuclei

Many studies have now been made of levels in odd-mass nuclei located in the "vibrational" regions ($0.1 \leq |\beta| \leq 0.25$). Rather unambiguous decoupled bands have been seen in the Au region[7]), the light Gd-Yb region[5,8]), the La region[6,9]), and the Ru-Pd region[10,11]). The alternative rotational-bandlike levels have been seen in light Tℓ nuclei[7]) and in the light Ce-Nd nuclei[12]). For both types of band there may be other regions, as a careful survey was not made. The point is that a rather large amount of evidence has already been accumulated showing that the expectations outlined in the previous section do often occur in nuclei. Rather than surveying all these regions, I have chosen one, the La-Ce region, to illustrate the application of these ideas to the observed levels.

3.1 The La-Ce Region

A portion of the Nilsson diagram for protons is shown in fig. 3, where some of the orbitals have been fully drawn, and others have not. For the La nuclei, with 7 protons beyond the closed shell at 50 (at $\beta = 0$, this closed shell is at the bottom of fig. 3) and deformations 0.15 - 0.25 (for mass numbers 137 - 125), the $h_{11/2}$ orbital is essentially empty in all cases. Thus, the simple one-particle calculations of fig. 2 should apply, and for prolate shapes (anticipating the results), decoupled bands should occur for all these La nuclei. Now consider the neutrons in ^{135}Ce,^{137}Nd(77) and ^{133}Ce,^{135}Nd(75), where $\beta \sim 0.15 - 0.20$. Figure 3 can also give an estimate for neutrons in this region; the 82 closed shell comes between the $h_{9/2}$ and $s_{1/2}$ orbitals. If the nuclei are prolate, the N = 77 cases (with 5 holes in the 82 closed shell) will have one hole in the $h_{11/2}$ orbital, so that fig. 2 should be applicable except with the sign of β reversed. Thus, normal rotational-bandlike levels are expected, with a tendency for the levels,

after the first one (I = j), to be paired: j + 1 and j + 2; j + 3 and j + 4; ... . For the N = 75 nuclei (7 holes in the 82 shell) the Fermi level has dropped to around the 9/2 component of the $h_{11/2}$ orbital. This gives three holes in the $h_{11/2}$ orbital and fig. 2 does not apply. Appropriate calculations show that one expects a perturbed $\Omega = 9/2$ rotational band, where the j, j+2, j+4, ··· levels again lie anomalously low. Thus for prolate deformation a unique set of predictions can be made, and an equally unique and opposite set would be made for the oblate case.

The negative-parity La levels[6,9]) are shown in fig. 4, where they are compared with the levels in the even-even Ba isotope with one fewer proton. The correspondence in spin and energy of the odd-mass and even-even levels is remarkable, and comprises the first, and still perhaps the best, example of decoupled bands. Other features of these bands support this interpretation. The lack of population of other negative parity states argues against the weak-coupling scheme, which could otherwise explain these energies. The spectroscopic factors for population of the $11/2^-$ state in the (α,t) and (^{3}He,d) reactions vary from about 1.0 in ^{139}La to 0.4 in ^{131}La, in good accord with calculations[9]) like those of fig. 2. Also the dramatic drop in energy, as the mass number decreases, of the $11/2^-$ state relative to the positive parity states ($d_{5/2}$,$g_{7/2}$) in the La isotopes can be understood in this interpretation. All the known characteristics of these La levels support their assignment as decoupled $h_{11/2}$ bands.

In fig. 5 the levels recently determined[12]) for ^{135}Ce and ^{137}Nd are shown. The normal rotational-band order of the negative-parity levels is seen, but the perturbations favoring the j, j + 2, ..., levels are quite strong. This is qualitatively what is expected for a prolate shape; however, quantitatively the observed spacings are somewhat less

regular than calculated. This is in the direction that might be expected if there were some shape (γ) asymmetry, or softness toward such asymmetry, and the low-lying second 2+ state in the adjacent even-even nuclei show that this is very likely to be the case. Additional evidence that these nuclei are prolate comes from the large negative A_2 coefficients (~ -1.0) in the angular distributions of the M1 + E2 gamma rays in the $11/2^-$ band. This implies a negative sign for δ, the mixing ratio, and therefore a positive Q_0 (prolate), since $g_K - g_R$ will be negative for the $h_{11/2}$ neutron and the sign of δ is determined by the sign of $(g_K - g_R)/Q_0$. The level schemes for ^{133}Ce and ^{135}Nd are shown in fig. 6. They are also rotational-bandlike, have $9/2^-$ for the lowest spin rather than $11/2^-$, show more regular energy spacings than the previous set, and also have the large negative A_2 coefficients for the M1 + E2 transitions. All of these are in accord with expectations for a prolate shape, and show that these odd-neutron nuclei are behaving much as the particle-plus-rotor model would predict.

A question arises as to why a simple axially- symmetric particle-plus-rotor model should work so well in this La-Ce (or any other similar) region. It seems likely that many other features are involved in the core states; vibrational motions, asymmetric shapes, sizeable individual 2-particle amplitudes, etc. Part of the answer to this problem may have been given by Greiner[13]), who pointed out that in a wide variety of collective models the even-even yrast states (lowest-lying 0^+, 2^+, 4^+, ...) have a strong rotational character, even though the other lower-spin states do not. If an odd particle is coupled to these yrast states, it will, therefore, produce a particle-plus-rotor spectrum; and the odd-mass yrast states in this spectrum may not be much affected by the states based on all the non-yrast core states. Thus, the odd-mass yrast states will look

like particle-plus-rotor states; whereas, the lower spin states may not. This explanation could be true since one of the beautiful (limiting?) features of the (HI,xnγ) reactions is the high specificity for populating yrast states, thereby producing very little information about lower spin states. It will be of considerable interest to study these lower spin states, and also the states from lower-j orbitals where additional features may occur.

3.2 The Light Odd-Mass Er Nuclei

There are two reasons for discussing the light odd-mass Er nuclei. The first is that they show very clearly the transition from a deformation-aligned region to a rotation-aligned region. The second is that they are involved in some of the arguments about even-even nuclei which will be made in the next section.

In fig. 7 the energy level spacings, in units of $\frac{\hbar^2}{2\mathfrak{J}}$, are shown for a decoupled band and for a strongly-coupled rotational band based on the $i_{13/2}$ orbital. The rotational spacings shown on the left are independent of Ω (except for 1/2); and also, the existence of possible lower band members is irrelevant to the present arguments. It is apparent that the decoupled band is very heavily compressed (by the Coriolis interactions), and a measure of this compression could serve as a measure of the extent of decoupling. If an average E_{2+} $(6\frac{\hbar^2}{2\mathfrak{J}})$ is determined from the adjacent even-even nuclei, then the 17/2 - 13/2 spacing divided by this E_{2+} would be 1.0 for a decoupled band, and 5.3 for a rotational band. Comparing the 21/2 - 17/2 spacing with the even-even 4 - 2 separation would give 1.0 and 2.9 for the two types of band. Thus an estimate can be made at any spin value of how decoupled an observed band is.

A plot of this odd-A-to-average-even-even transition energy ratio is shown in fig. 8 for the lowest band based on the $i_{13/2}$ orbital in the odd-mass Er isotopes. The decoupled-band limit for this ratio is always 1.0; whereas, the rotational band limit varies from about 5 to 2. For the 17/2 - 13/2 energy spacing the observed ratio drops monotonically from 3.6 for ^{167}Er ($\beta \sim 0.33$) to 1.0 for ^{157}Er ($\beta \sim 0.2$). This is just the trend expected; and it is caused both by the decrease in β and by a decrease in the Fermi level with mass number toward the $\Omega = 1/2$ state (the one-particle situation). The other important trend is with spin, I, and it is clear that the extent of decoupling increases with increasing I, as expected. Thus, the $i_{13/2}$ bands in these Er nuclei show very clearly the transition to the rotation-aligned coupling scheme. Note that ^{157}Er and ^{159}Er have essentially pure decoupled bands even for the lowest spins.

4. Even-Even Nuclei

An interesting new effect has recently been observed around $I \sim 16$ in the ground-state rotational band (yrast states) of some even-even rare-earth nuclei[14]). It is called "backbending", and an illustration of what this means is given in fig. 9. The main plot shows the yrast states of ^{162}Er on an energy vs. I plot, and although this looks rather ordinary, the slope has some distinct changes around I = 16. The insert shows the currently popular way to plot these data: as (essentially) the moment of inertia, $\mathcal{J}$, (defined from the transition energy) vs. the square of the rotational frequency, ω. The rotational frequency is proportional to the slope of the main curve, and it is approximated as one-half the transition energy in fig. 9. The slope changes appear clearly on this plot, and the origin of the name, backbending, is obvious. The effect is not a very dramatic one on the main plot but, on the other hand, $\hbar\omega$ (the transition energy) is directly measured so that the backbend is unmistakeable and quite likely indicative of some interesting phenomenon.

A process that might cause backbending is illustrated in fig. 10. The ground-state band, labeled as the paired vacuum state $|\tilde{0}\rangle$, is shown to be crossed by another band, the lower one of which in fig. 10 is labeled "decoupled". The band implied here is a two-quasiparticle one, where the first quasiparticle has the maximum angular-momentum projection on the rotation axis, $\alpha = j = 13/2$, and the second quasiparticle has the maximum remaining projection on that axis, $\alpha = j - 1$. This is written in the usual second-quantization notation as $\alpha^{\dagger}_{13/2}\alpha^{\dagger}_{11/2}|\tilde{0}\rangle$, where $\alpha^{\dagger}$ is a creation operator for quasiparticles and the subscript refers to the rotation-aligned quantum number called (somewhat unfortunately in this context) α. Such a band crossing can produce all the effects presently

known to occur in the backbending region[15]). These include backbending in the ground band (and also in the β-band) and the various features of the population of these states following (HI,xnγ) reactions: a) the amount of population observed for each rotational level with various projectiles on different types of nuclei, b) the fast collective E2 transitions above, through and below the intersection region, and c) the lack of any observed transitions above the intersection region. The explanation of these properties will not be discussed, as they already are rather well known. There is, at present, a considerable amount of evidence that a band crossing is involved in backbending. Furthermore, all the data presently known (by me) can be at least qualitatively accounted for if the crossing band is assumed to be this two-quasiparticle rotation-aligned band.

Another possible explanation of backbending is that the pairing correlations in the nucleus may be rather suddenly quenched at high rotational frequencies due to the increasing Coriolis force. Such a model can be schematically represented by a crossing of the paired ground band by a band based on the unpaired vacuum state, $|0\rangle$, shown also in fig. 10. Such a collapse of pairing was predicted by Mottelson and Valatin[16]) to occur at about these spin values. This pairing collapse has recently been the subject of much study, and three recent review articles[17-19]) discuss it. The next speaker, Prof. Z. Szymanski, will report on this subject. While other causes for backbending have been proposed, these two, rotation alignment and pairing collapse, have received the most attention; and at present no definitive experimental test has been proposed to distinguish between them. The remainder of this section will consist of an attempt to propose and apply such a test.

The essence of this test is to determine the effect of an odd decoupled $i_{13/2}$ neutron on the backbending process. It has been shown in previous sections

that such bands occur in the light Er nuclei, and have energy spacings very similar to those of the adjacent even-even nuclei. These even-even nuclei backbend, and the proposed test is to predict and measure the odd-mass behavior in this spin region.

The prediction of the pairing-collapse model about backbending in a decoupled $i_{13/2}$ band can be stated very simply. An odd particle reduces the pairing correlations due to blocking effects, and thus the pairing collapses at a lower rotational frequency. This statement can be illustrated in fig. 11. The solid lines show the even-even situation based on this model: the paired vacuum state intersecting the unpaired vacuum state. The dashed lines show the odd-mass situation. For the unpaired case, the one particle state, $a^{\dagger}_{13/2}|0\rangle$, and the even-even vacuum state, $|0\rangle$, coincide as shown, provided: 1) the vacuum is assumed to be the average of the two nuclei adjacent to the odd-mass nucleus; 2) the decoupled $i_{13/2}$ state lies at the Fermi surface, and 3) the level density is reasonably large. However, in the paired case the one-quasiparticle state always occurs higher in energy than the vacuum state by the odd-even mass difference, Δ. The dashed line in fig. 11 for the odd-mass band with pairing is, therefore, raised in energy by this amount - taken to be 0.8 MeV. As a result, the intersection with the unpaired band is seen to occur at <u>lower</u> spin and also at lower rotational frequency (slope).

An opposite change is expected in the rotation-alignment picture as is illustrated in fig. 12. Again the solid lines represent the even-even situation: the paired vacuum state crossing the rotation-aligned two-quasiparticle state. Adding an odd particle to each of these states raises both of them by the energy, Δ, due to pairing effects; but this can be ignored since only the relative energy (crossing point) is of interest. The one-quasiparticle state then coincides in energy with the paired vacuum state as shown in fig. 12. However, the same decoupled

two-quasiparticle state involved in the even-even case cannot be made in the odd-mass case due to the Pauli principle. The odd neutron is already occupying the $\alpha = 13/2$ state. The most favorable states available to the broken pair are then $\alpha = 11/2$ and $\alpha = 9/2$; so that, the three quasiparticle state becomes: $\alpha^{\dagger}_{13/2}\,\alpha^{\dagger}_{11/2}\,\alpha^{\dagger}_{9/2}|\tilde{0}\rangle$. The energy difference between the one- and three-quasiparticle state is larger than that between the zero- and two-quasiparticle states because (1) the $\alpha = 9/2$ state is less favorable energetically than is the $\alpha = 13/2$ state, and (2) the additional angular momentum gained by breaking the pair is only 10 $\hbar$ rather than 12 $\hbar$, so that 2 $\hbar$ more of core rotational angular momentum is required. The sum of these two effects is about 1 MeV, so that the intersection should come at <u>higher</u> spin and rotational frequency as shown in fig. 12. Note that if the odd particle were not in the $i_{13/2}$ orbital, there would be no predicted change in the intersection point. To obtain the situation in fig. 12, the odd particle must be one of those involved in the even-even two-quasiparticle state.

In order to determine which prediction is correct, additional experiments were made to extend the data in the decoupled bands of ^{157,159}Er to higher spin values[20]). The backbending curves for ^{156}Er and ^{158}Er are shown in fig. 13, where the decoupled band in ^{157}Er has also been plotted. If ^{157}Er backbends, it clearly does so only at higher rotational frequencies (and spin values) than its even-even neighbors. The situation for ^{158,159,160}Er is shown to be very similar in fig. 14, except that ^{159}Er is not quite completely decoupled at the lowest (13/2,17/2) spin values. This failure of the odd-mass bands to backbend is in agreement with the rotation-alignment explanation of backbending, and in apparent disagreement with the pairing-collapse explanation.

A more sensitive way to present these same data is shown in fig. 15. Here we have plotted the ratio of transition energy in the odd-mass nucleus ($E_{I+j} - E_{I+j-2}$) to that in the even-even nucleus ($E_I - E_{I-2}$) <u>versus</u> I. Prior to the backbend region ($I \lesssim 12$), both odd-mass nuclei seem to be converging to a value of about 1.1. As the even-even backbend occurs, however, ($I = 14$) the ratio rises sharply since the odd-mass bands to not experience the same drop in transition energy. This sharp rise at $I = 14$ is very clear in both cases.

Probably the greatest uncertainty in this test arises from the possibility that an entirely unforeseen effect is causing the odd-mass bands not to backbend. This can be checked by looking at the $h_{11/2}$ decoupled bands in ^{157}Ho and ^{159}Ho. Since the rotation-alignment picture describes the crossing band as composed mainly of $i_{13/2}$ neutrons, the blocking of a proton orbital should have much less, if any, effect on the backbending. Thus, the decoupled bands in ^{157,159}Ho should backbend like the even-even nuclei, and preliminary data[21]) indicates that they do. If this proves to be the case, it will not only confirm the present test, but also provide a means to analyze which configurations are important in the band intersecting the ground band. This could be useful in the Os region, for example, where it is not clear, even if the rotation-alignment picture is correct, whether $i_{13/2}$ neutrons or $h_{9/2}$ protons are mainly responsible for the backbending.

5. Conclusion

In a number of odd-mass nuclei evidence has been presented showing that the particle-plus-rotor model gives a reasonable description of the yrast states in the range $|\beta| \gtrsim 0.1$. This is a considerable extension, toward smaller β values, of the expected range of validity of this model. It is not clear at present whether this description is valid only for the high-spin yrast states, or whether lower-spin states in these nuclei are also explained. Low-lying high-spin states, in general, tend to have the odd-particle angular momentum, j, aligned with that of the rotating core. This suggests a coupling scheme where α, the projection of j on the rotation axis, is a good quantum number. Such a rotation-aligned coupling scheme has been discussed and describes rather well the yrast states in many odd-mass nuclei. This coupling scheme could be expected to apply to lower spin states under certain (rather common) conditions, and it is at present a challenge to find the proper experiments to test this.

In the even-even nuclei the rotation-aligned scheme may also play an important role. It has been suggested that backbending in the light rare-earth region may be just the intersection of the ground band with such a rotation-aligned two-quasiparticle state composed of $i_{13/2}$ neutrons. A test, based on backbending in odd-mass nuclei, suggests that this explanation (rather than the pairing-collapse explanation) is, indeed, correct in the light Er nuclei. Whether this will prove to be the case in other regions is not yet clear.

Acknowledgments

I am indebted to Drs. R. M. Diamond, S. G. Nilsson, and P. Kleinheinz for many discussions on these subjects. I would like to thank them and Drs. J. O. Rasmussen and D. Proetel for their comments on this manuscript.

References

1) A. Bohr, Dan. Mat. Fys. Medd. 26 (1952) 14

2) F. S. Stephens, R. M. Diamond, and S. G. Nilsson, Phys. Letters 44B (1973) 429

3) A. de-Shalit, Phys. Rev. 122 (1961) 1530

4) S. G. Nilsson, Dan. Mat. Fys. Medd. 29 (1955) no. 16

5) F. S. Stephens, 5th Summer School on Nuclear Physics, Instytut Badan Jadrowych, Report "P", No. 1447/I/PL, Warsaw, Poland (1972)

6) F. S. Stephens, R. M. Diamond, J. R. Leigh, T. Kammuri, and K. Nakai, Phys. Rev. Letters 29 (1972) 438

7) F. S. Stephens, R. M. Diamond, D. Benson, Jr., and M. R. Maier, Phys. Rev. C7 (1973) 2163

8) P. Kleinheinz, R. Sheline, M. R. Maier, R. M. Diamond, and F. S. Stephens, to be published (1973)

9) K. Nakai, P. Kleinheinz, J. R. Leigh, K. H. Maier, F. S. Stephens, and R. M. Diamond, Phys. Letters 44B (1973) 443; P. Kleinheinz, S. M. Harris, G. Løvhøiden, and K. Nakai, BAPS 17 (1972) 898

10) C. M. Lederer, J. M. Jaklevic, and J. M. Hollander, Nucl. Phys. A169 (1971) 489

11) P. C. Simms, F. A. Rickey, and J. R. Tesmer, Phys. Rev. Letters 30 (1973) 710

12) J. Gizon, A. Gizon, M. R. Maier, R. M. Diamond, and F. S. Stephens, submitted to Nucl. Phys. (1973)

13) W. Greiner, private communication (1972)

14) A. Johnson, H. Ryde, and J. Sztarkier, Phys. Letters 34B (1971) 605

15) F. S. Stephens and R. S. Simon, Nucl. Phys. A183 (1972) 257

16) B. R. Mottelson and J. G. Valatin, Phys. Rev. Letters 5 (1960) 511

17) A. Johnson and Z. Szymanski, Physics Reports (Section C of Phys. Letters) 7 (1973) 181

18) K. Kumar, preprint (1972), to be published in Physica Scripta (Sweden)

19) R. A. Sorensen, preprint (1973)

20) E. Grosse, F. S. Stephens, and R. M. Diamond, to be published (1973)

21) E. Grosse, F. S. Stephens, and R. M. Diamond, unpublished data (1973)

Figure Captions

Fig. 1. Schematic vector diagrams illustrating the deformation-aligned coupling scheme (above) and the rotation-aligned coupling scheme (below). The two types of wave function are also indicated.

Fig. 2. The results of diagonalizing eq. (6) for the $h_{11/2}$ orbital at various β values showing all the yrast states up to I = 23/2 (the second-lowest I = 11/2 state is also shown). The ordinate is the difference between the eigenvalue and that of the lowest I = 11/2 state, in units of E_{2^+}.

Fig. 3. A portion of the Nilsson diagram for protons, where only the $h_{11/2}$ and $h_{9/2}$ orbitals have been fully drawn.

Fig. 4. A comparison of the negative parity bands in the odd-mass La isotopes with the ground band in the neighboring Ba nuclei. In most cases (energy zero in parentheses) the La $11/2^-$ level is not the ground state and its energy has been subtracted from all levels shown for that isotope.

Fig. 5. Energy levels in ^{135}Ce and ^{137}Nd. The transitions in the $11/2^-$ bands are shown as solid; whereas, the others are open. The width of the arrows indicates the amount of population following the (HI,xnγ) reaction.

Fig. 6. Energy levels in ^{133}Ce and ^{135}Nd. The transitions in the $9/2^-$ bands are shown as solid; whereas, the others are open.

Fig. 7. Level spacings, in units of $\hbar^2/2\mathcal{J}$, for an $i_{13/2}$ particle in a normal rotational band (left) and in a decoupled band (right).

Fig. 8. The ratio of $\Delta E(I + 2 \rightarrow I)$ in an odd-mass nucleus divided by the average of the corresponding transition energies in the adjacent even-even nuclei $\Delta E(I + 2 - j \rightarrow I - j)$, is plotted against mass number for the light Er nuclei. The rotational-band and decoupled-band limits are shown together with the data for the first four such transitions in the lowest-energy $i_{13/2}$ band.

Fig. 9. A plot of energy vs. I for the ground-band rotational levels in ^{162}Er. The insert shows the same data in the type of plot generally used to show backbending behavior.

Fig. 10. An energy vs. I plot showing the paired ground-band in an even-even nucleus, $|\tilde{0}\rangle$, intersecting either the "decoupled" two-quasiparticle band or a band based on the unpaired vacuum state $|0\rangle$. This last state refers to the same nucleus (particle number), but no pairing correlations (sharp Fermi surface).

Fig. 11. This plot shows the intersection points, based on the pairing-collapse model, of the ground band with the unpaired excited band in: 1) an even-even nucleus (solid lines) and 2) an odd-mass nucleus with a decoupled $i_{13/2}$ odd particle (dashed lines). Note that the subscript on the creation operators ($\alpha^\dagger$ or $a^\dagger$) refers to the rotation-alignment quantum number, α.

Fig. 12. This plot shows the intersection points, based on the rotation-alignment model, of the ground band with the broken-pair excited band in: 1) an even-even nucleus (solid lines) and 2) an odd-mass nucleus with a decoupled $i_{13/2}$ odd particle (dashed lines). The subscripts on the quasiparticle creation operators ($\alpha^\dagger$) refer to the rotation-alignment quantum number, α.

Fig. 13. Conventional backbending plots for ^{156,158}Er, and for the decoupled band in ^{157}Er. We have used: $2\mathcal{J}/\hbar^2 = (4I' - 2)/(E_I - E_{I-2})$ and $\hbar\omega = (E_I - E_{I-2})/2$, where $I' = I$ for the even-even nuclei and $I' = I - j$ for the decoupled band in the odd-mass nucleus.

Fig. 14. Conventional backbending plots for ^{158,160}Er and for the decoupled band in ^{159}Er. See caption to fig. 13.

Fig. 15. Plot of the decoupled band transition energy divided by the corresponding even-even energy vs. I for ^{157,159}Er. The even-even value used is the average of the two adjacent nuclei.

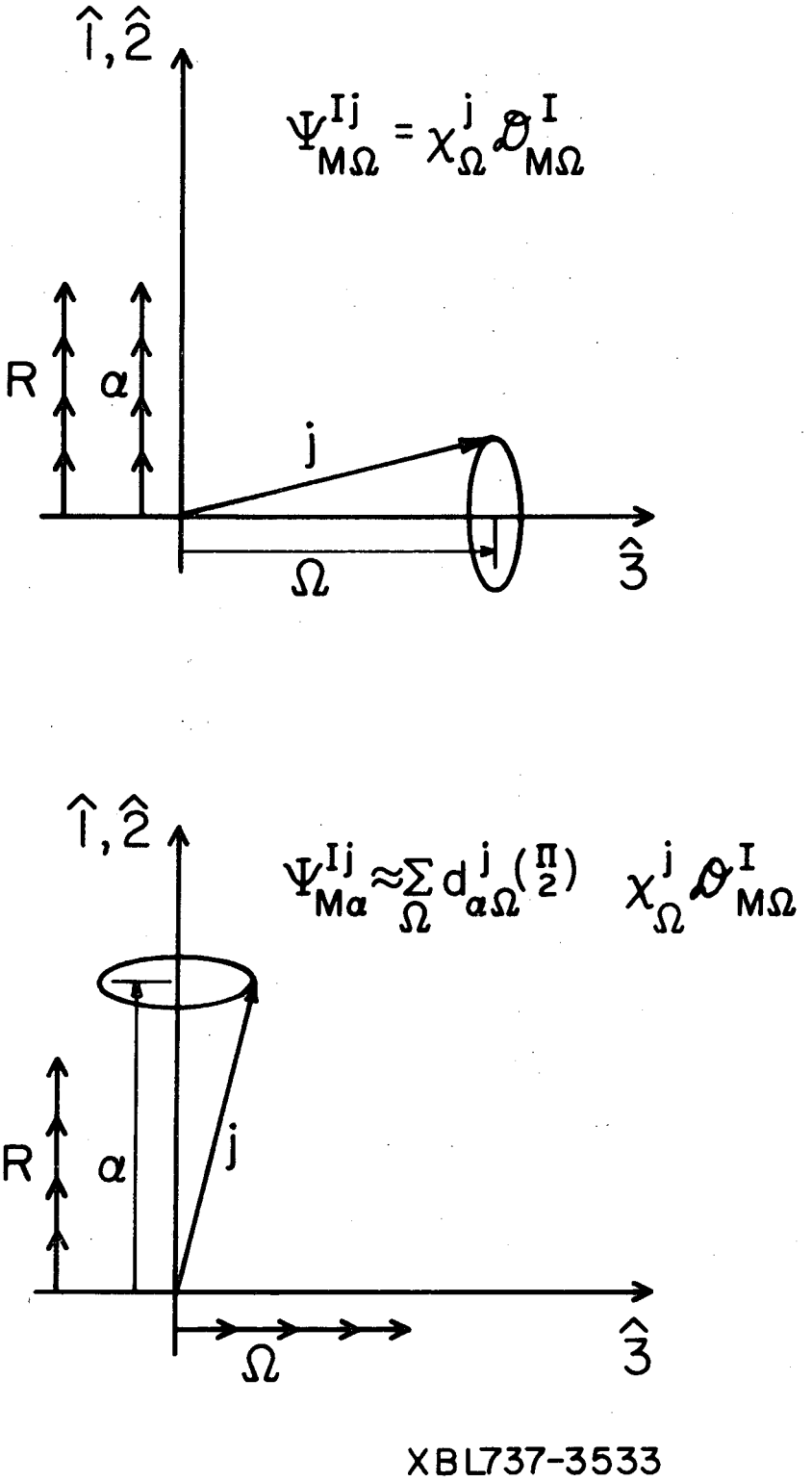
$\hat{1},\hat{2}$
$\Psi^{Ij}_{M\Omega} = \chi^{j}_{\Omega}\mathcal{D}^{I}_{M\Omega}$
R
α
j
Ω
$\hat{3}$
$\hat{1},\hat{2}$
$\Psi^{Ij}_{M\alpha} \approx \sum_{\Omega} d^{j}_{\alpha\Omega}(\frac{\pi}{2})\ \chi^{j}_{\Omega}\mathcal{D}^{I}_{M\Omega}$
R
α
j
Ω
$\hat{3}$
XBL737-3533

Fig. 1

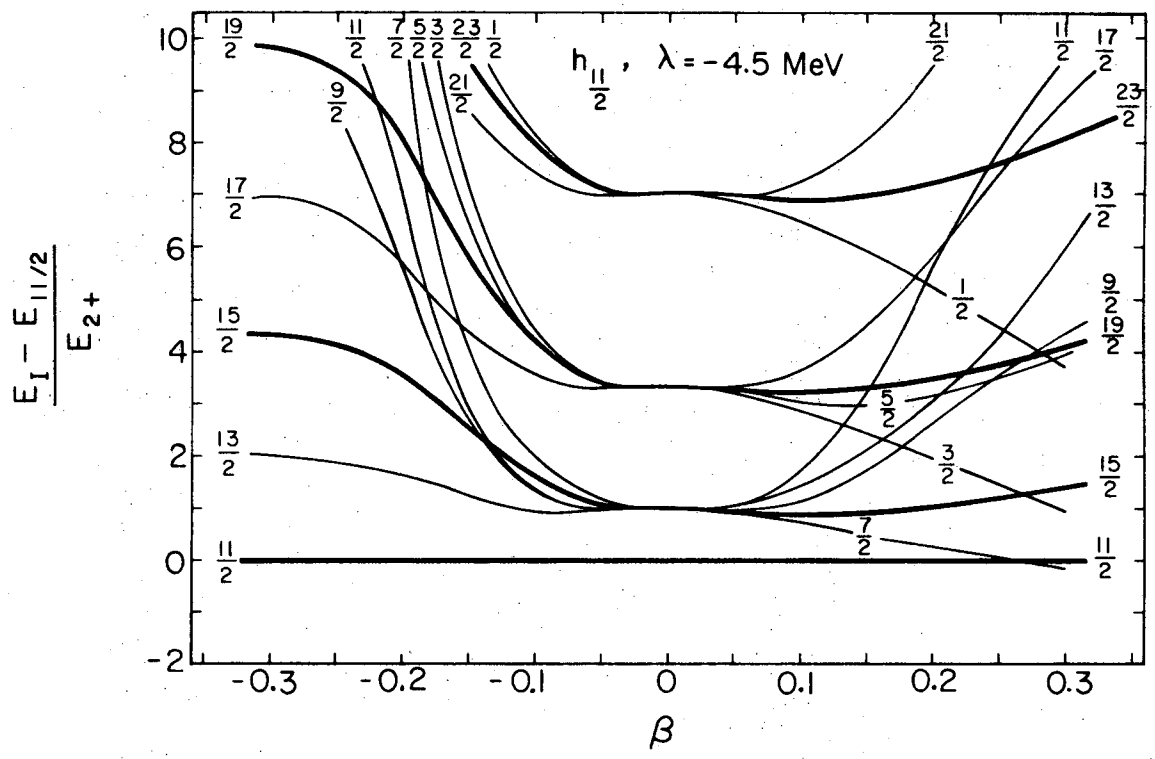

XBL 728-3728

Fig. 2

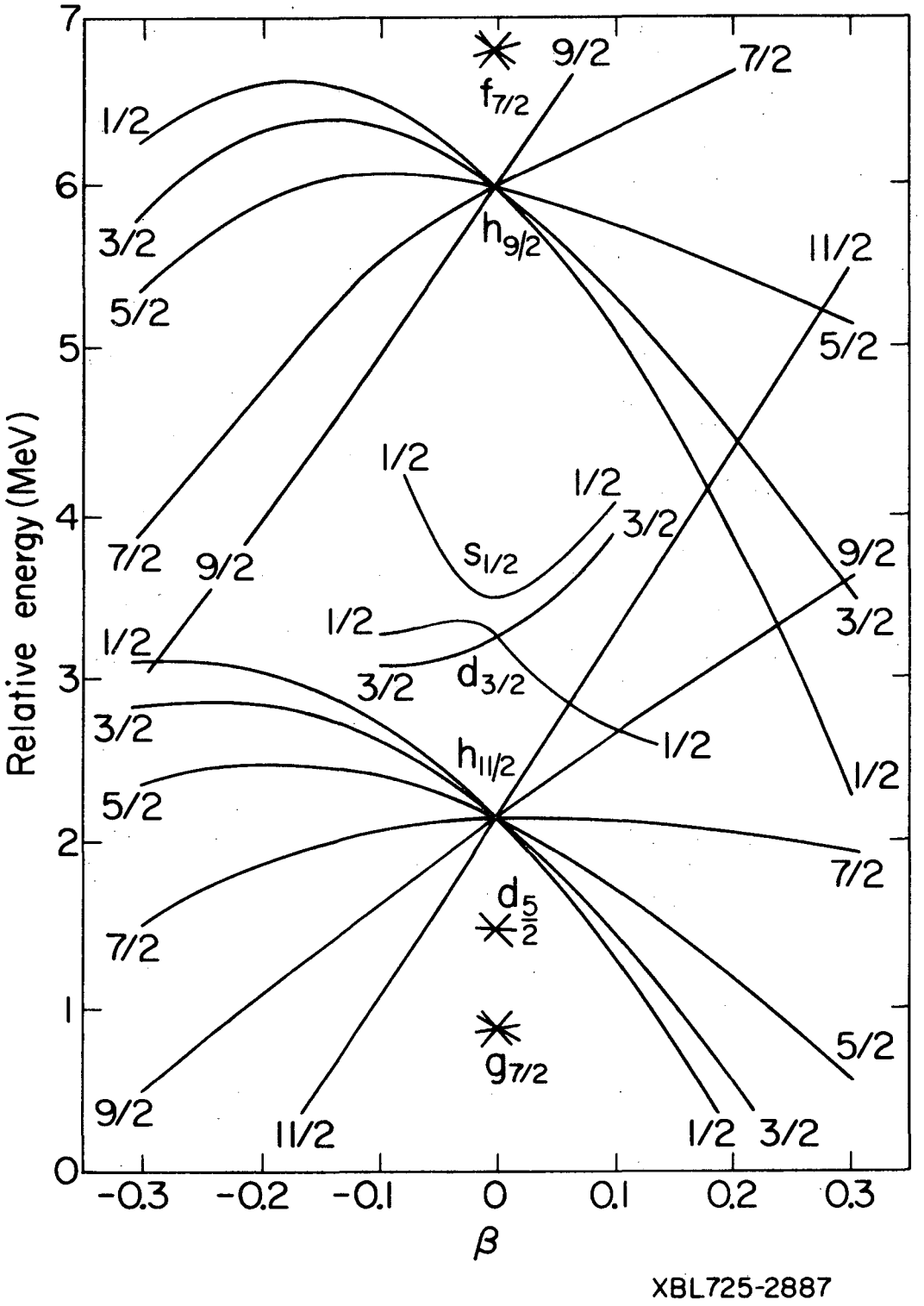
Relative energy (MeV)
β
$f_{7/2}$
$h_{9/2}$
$s_{1/2}$
$d_{3/2}$
$h_{11/2}$
$d_{\frac{5}{2}}$
$g_{7/2}$
XBL725-2887

Fig. 3

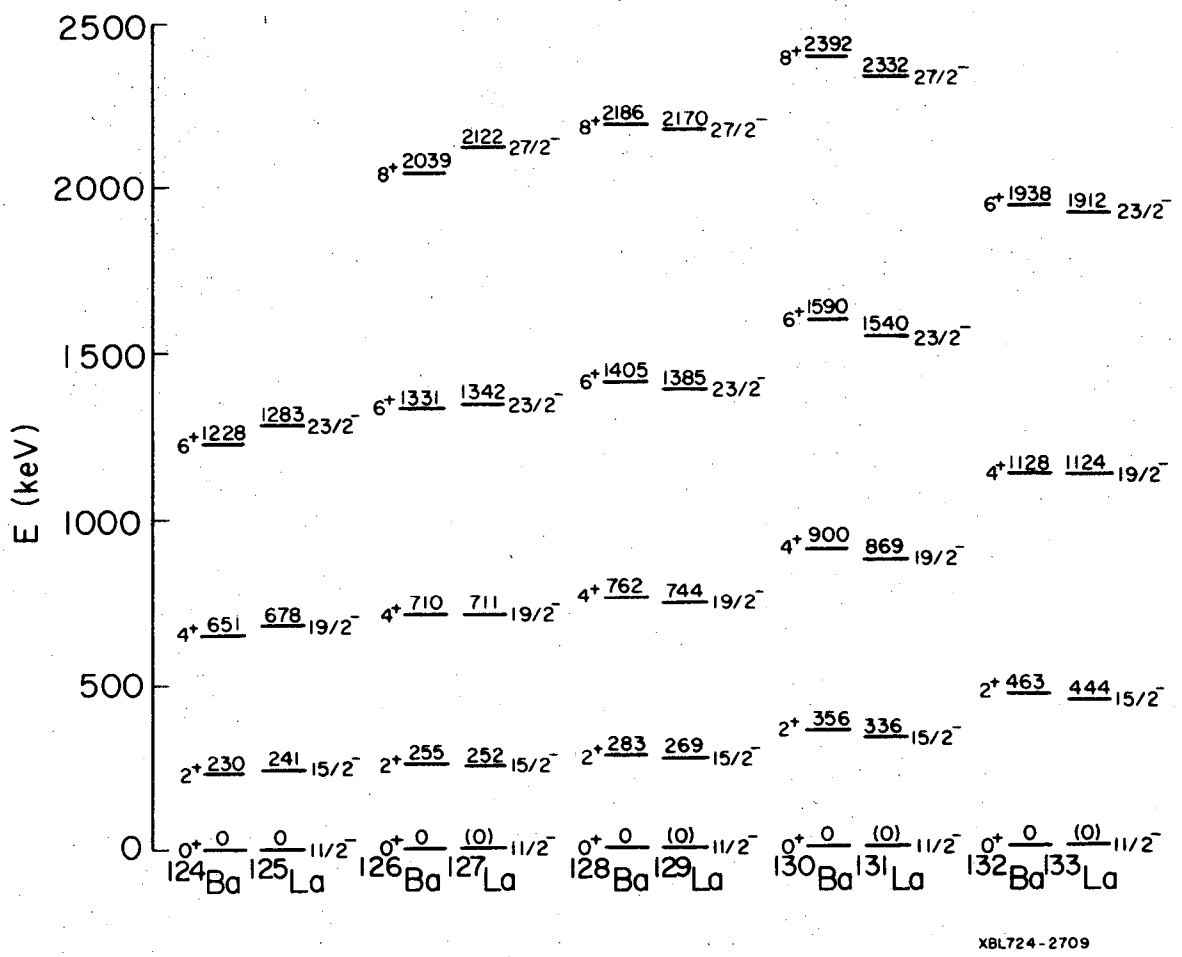
E (keV)
2500
2000
1500
1000
500
0
^{124}Ba
^{125}La
^{126}Ba
^{127}La
^{128}Ba
^{129}La
^{130}Ba
^{131}La
^{132}Ba
^{133}La
XBL724-2709

Fig. 4

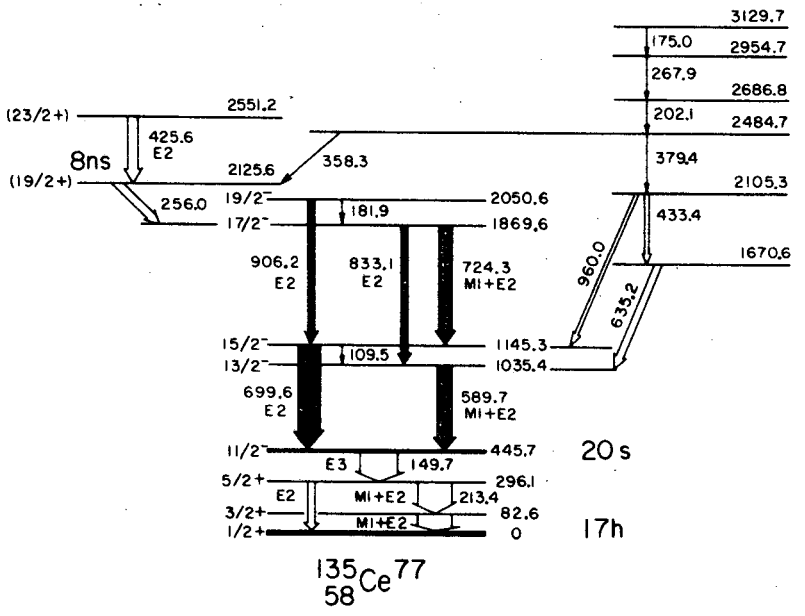

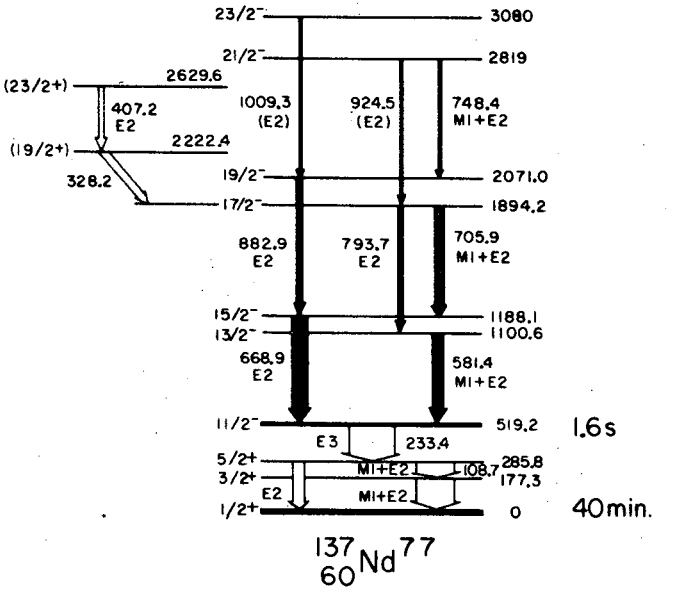

XBL 736-3107

Fig. 5

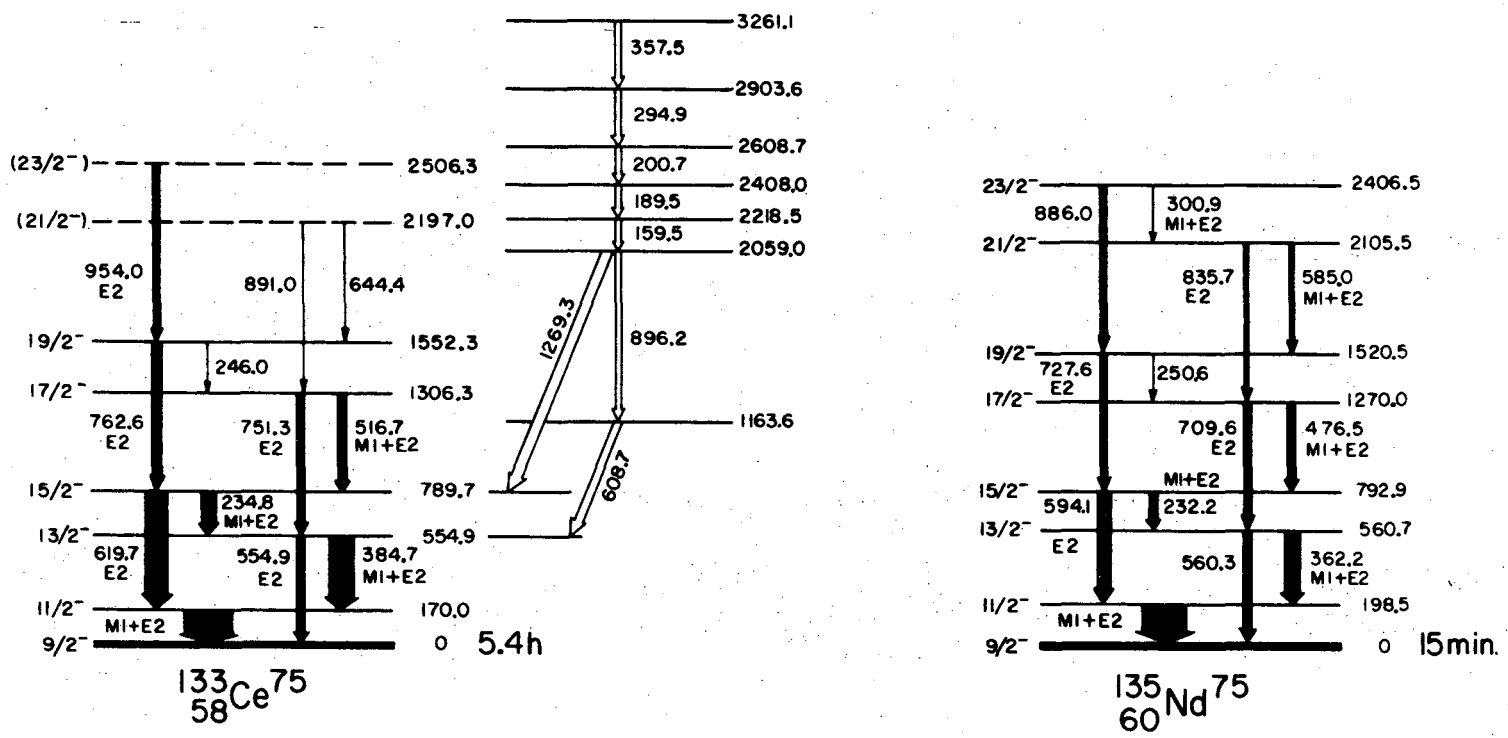
(23/2⁻) 2506.3
(21/2⁻) 2197.0
19/2⁻ 1552.3
17/2⁻ 1306.3
15/2⁻ 789.7
13/2⁻ 554.9
11/2⁻ 170.0
9/2⁻ 0 5.4h
954.0 E2
891.0
644.4
246.0
762.6 E2
751.3 E2
516.7 M1+E2
234.8 M1+E2
619.7 E2
554.9 E2
384.7 M1+E2
M1+E2
133 58 Ce 75
3261.1
2903.6
2608.7
2408.0
2218.5
2059.0
1163.6
357.5
294.9
200.7
189.5
159.5
1269.3
896.2
608.7
23/2⁻ 2406.5
21/2⁻ 2105.5
19/2⁻ 1520.5
17/2⁻ 1270.0
15/2⁻ 792.9
13/2⁻ 560.7
11/2⁻ 198.5
9/2⁻ 0 15min.
886.0
300.9 M1+E2
835.7 E2
585.0 M1+E2
727.6 E2
250.6
709.6 E2
476.5 M1+E2
M1+E2
594.1 E2
232.2
560.3
362.2 M1+E2
M1+E2
135 60 Nd 75
XBL736-3108

Fig. 6

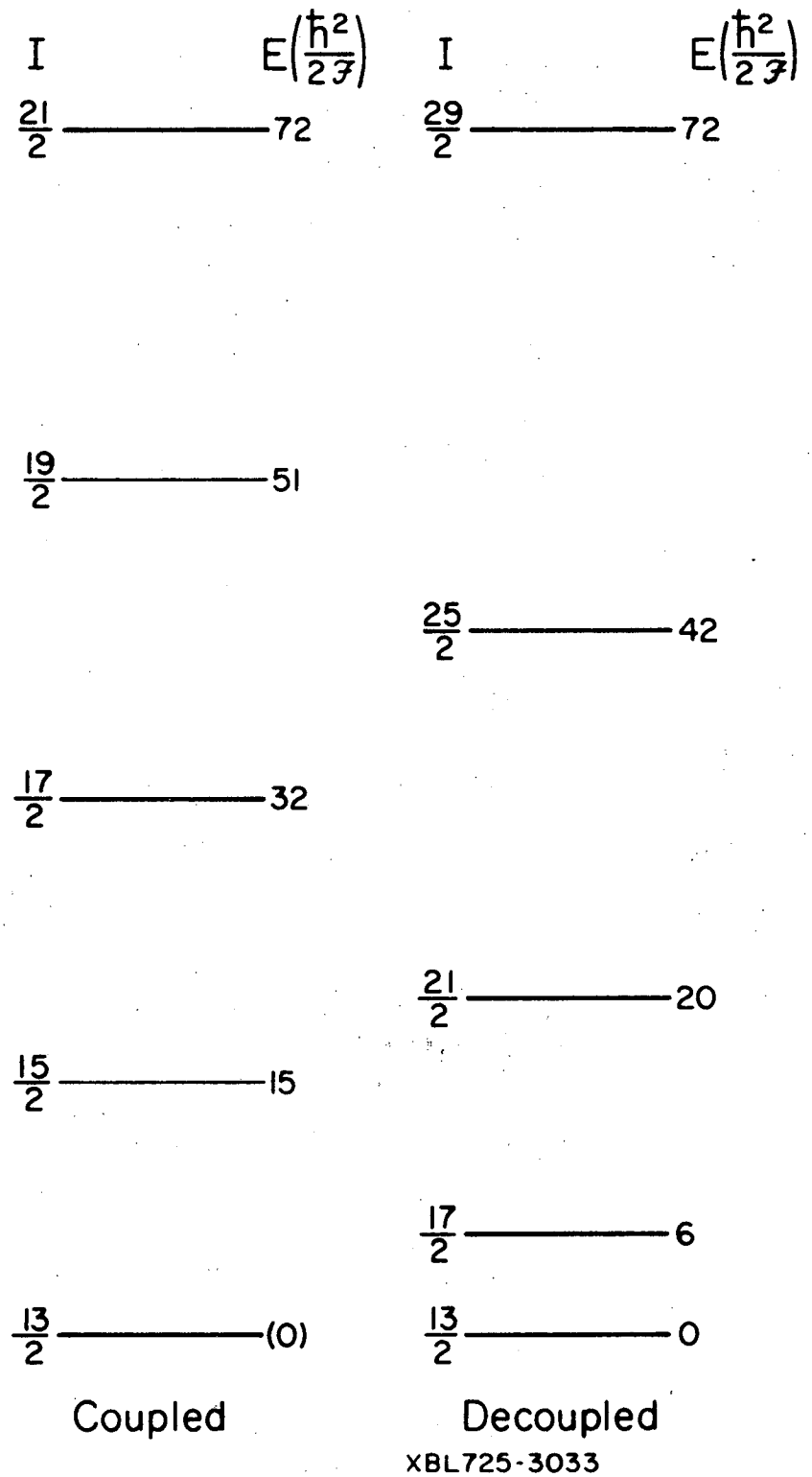
I
E(ħ²/2𝒥)
21/2
72
19/2
51
17/2
32
15/2
15
13/2
(0)
Coupled
I
E(ħ²/2𝒥)
29/2
72
25/2
42
21/2
20
17/2
6
13/2
0
Decoupled
XBL725-3033

Fig. 7

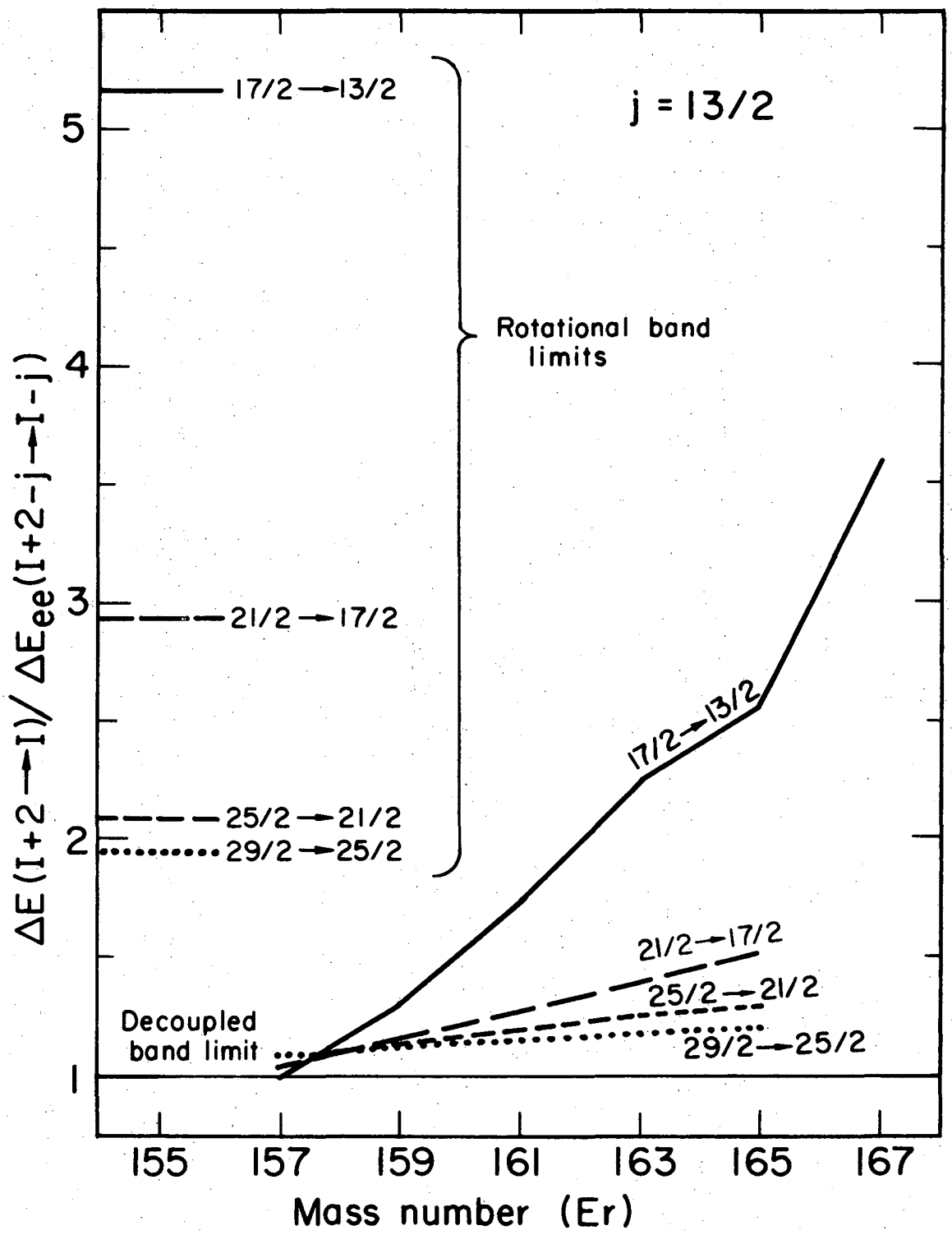

XBL731-2028

Fig. 8

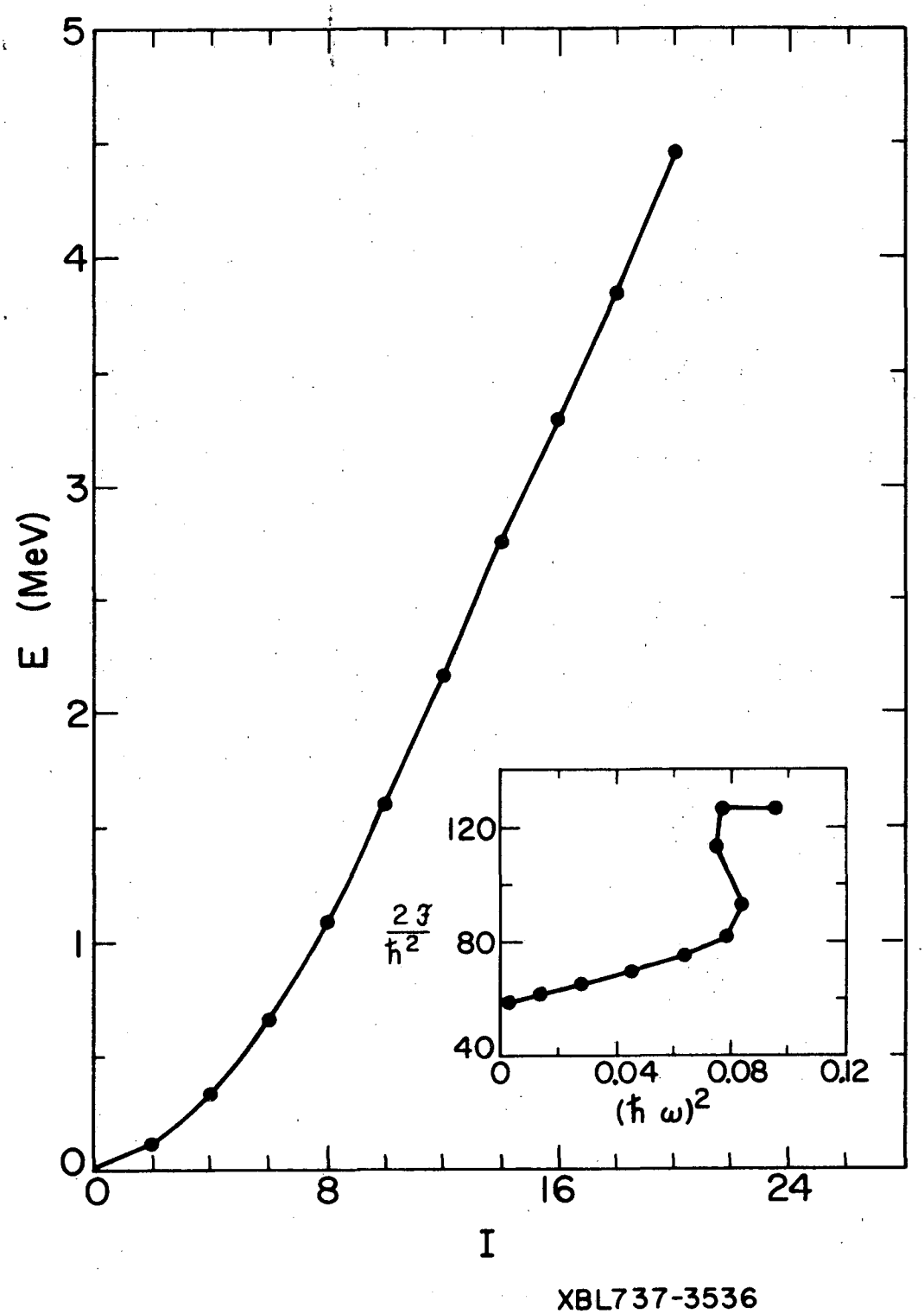
E (MeV)
I
0
1
2
3
4
5
0
8
16
24
$\frac{2\mathcal{J}}{\hbar^2}$
40
80
120
0
0.04
0.08
0.12
$(\hbar\omega)^2$
XBL737-3536

Fig. 9

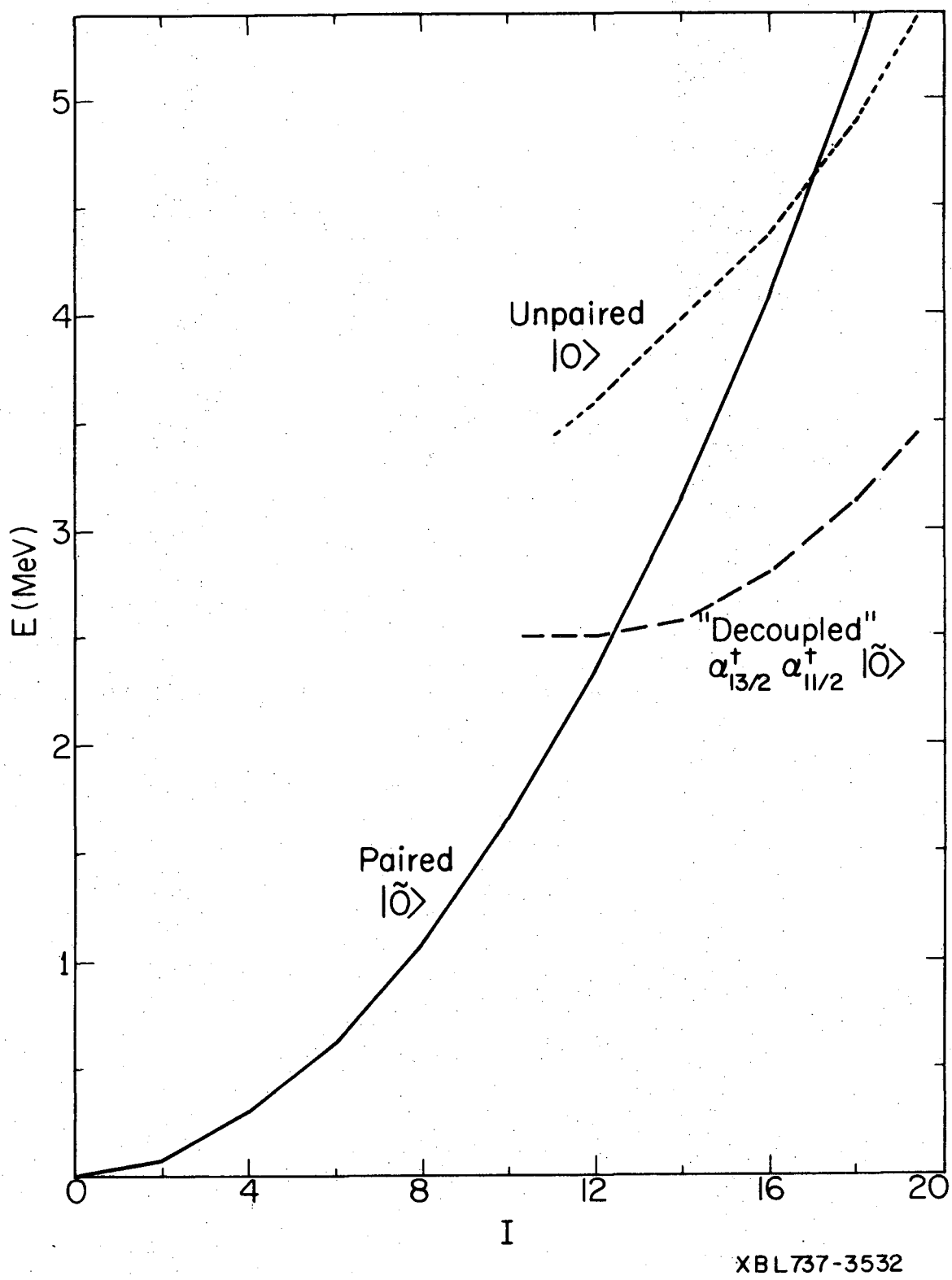
5
4
3
2
1
E (MeV)
0
4
8
12
16
20
I
Unpaired
|0⟩
"Decoupled"
$\alpha^{\dagger}_{13/2}\,\alpha^{\dagger}_{11/2}\,|\tilde{0}\rangle$
Paired
$|\tilde{0}\rangle$
XBL737-3532

Fig. 10

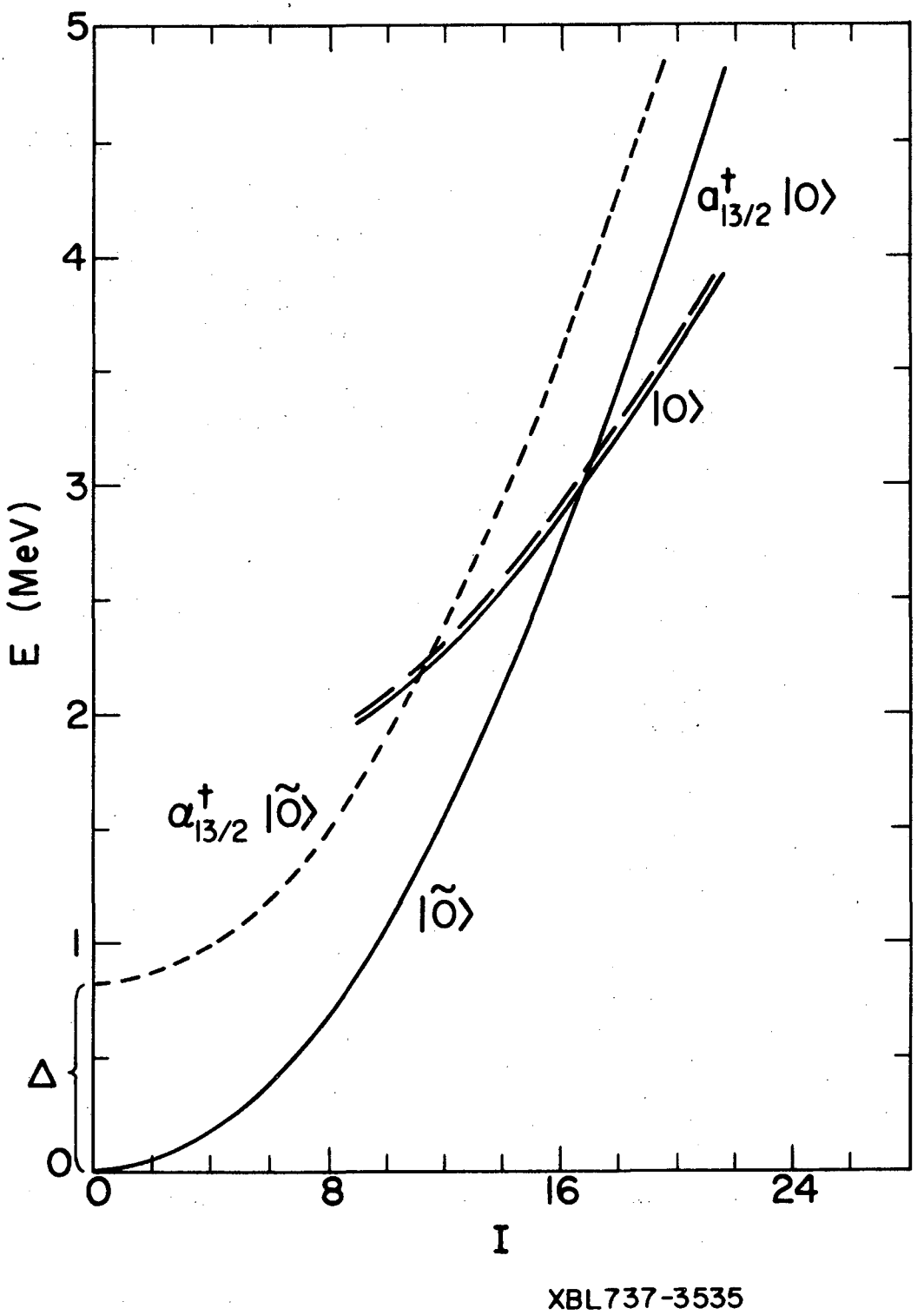
5
4
3
2
1
0
E (MeV)
Δ
0
8
16
24
I
$a^{\dagger}_{13/2}|0\rangle$
$|0\rangle$
$a^{\dagger}_{13/2}|\tilde{0}\rangle$
$|\tilde{0}\rangle$
XBL737-3535

Fig. 11

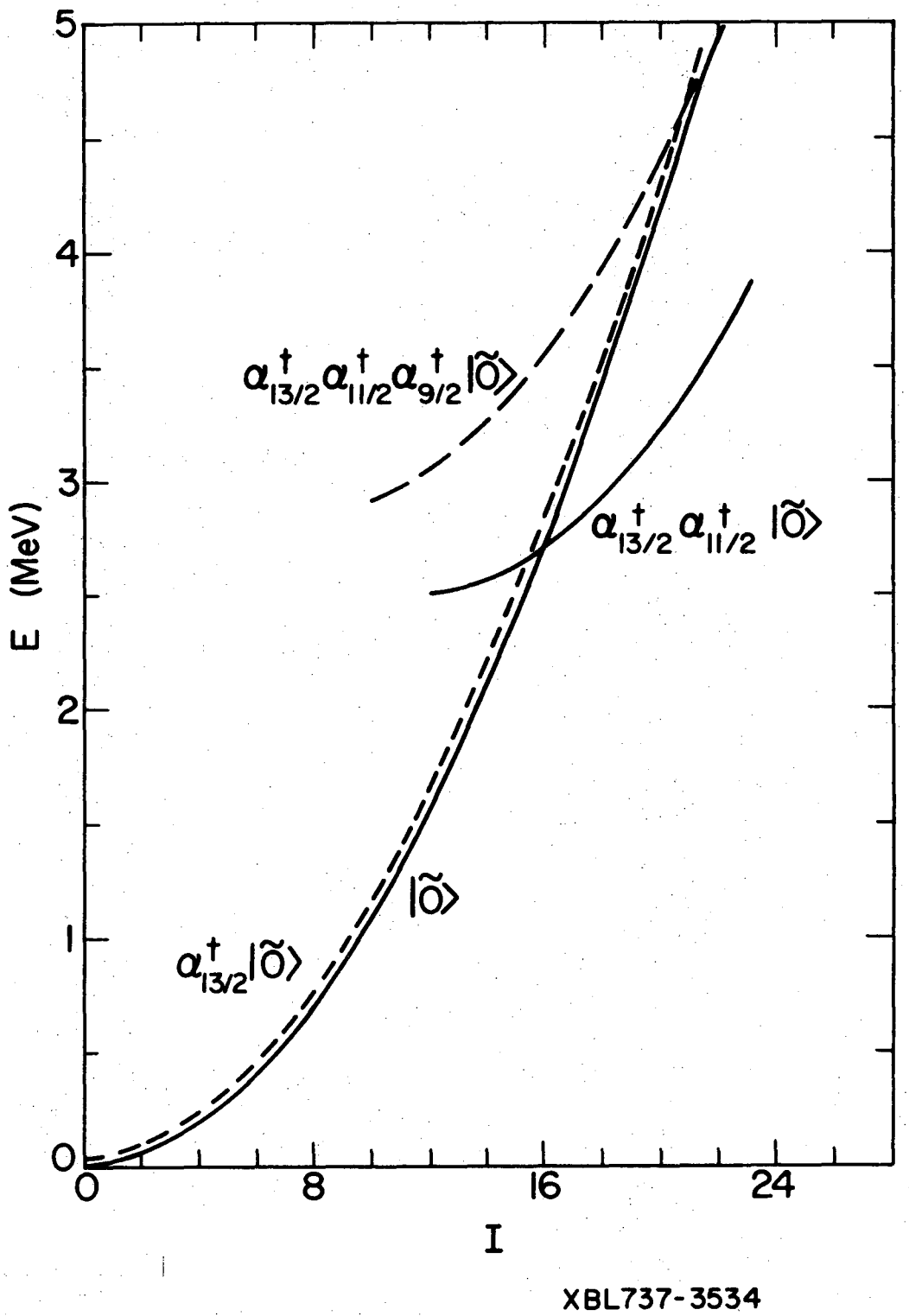
5
4
3
2
1
0
E (MeV)
0
8
16
24
I
$\alpha^\dagger_{13/2}\alpha^\dagger_{11/2}\alpha^\dagger_{9/2}|\tilde{0}\rangle$
$\alpha^\dagger_{13/2}\alpha^\dagger_{11/2}|\tilde{0}\rangle$
$|\tilde{0}\rangle$
$\alpha^\dagger_{13/2}|\tilde{0}\rangle$
XBL737-3534

Fig. 12

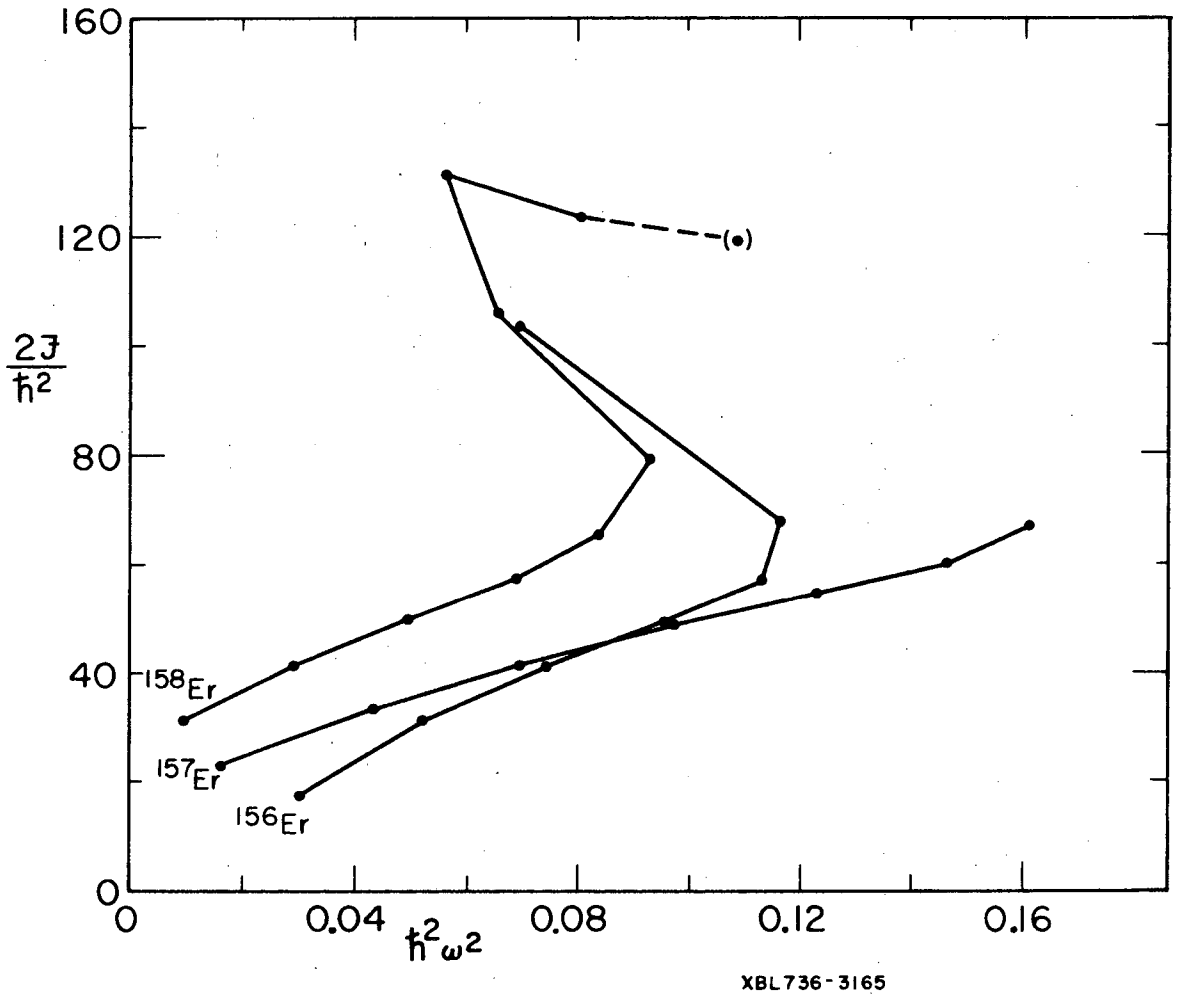
160
120
80
40
0
$\frac{2\mathcal{J}}{\hbar^2}$
(•)
158Er
157Er
156Er
0
0.04
0.08
0.12
0.16
$\hbar^2\omega^2$
XBL736-3165

Fig. 13

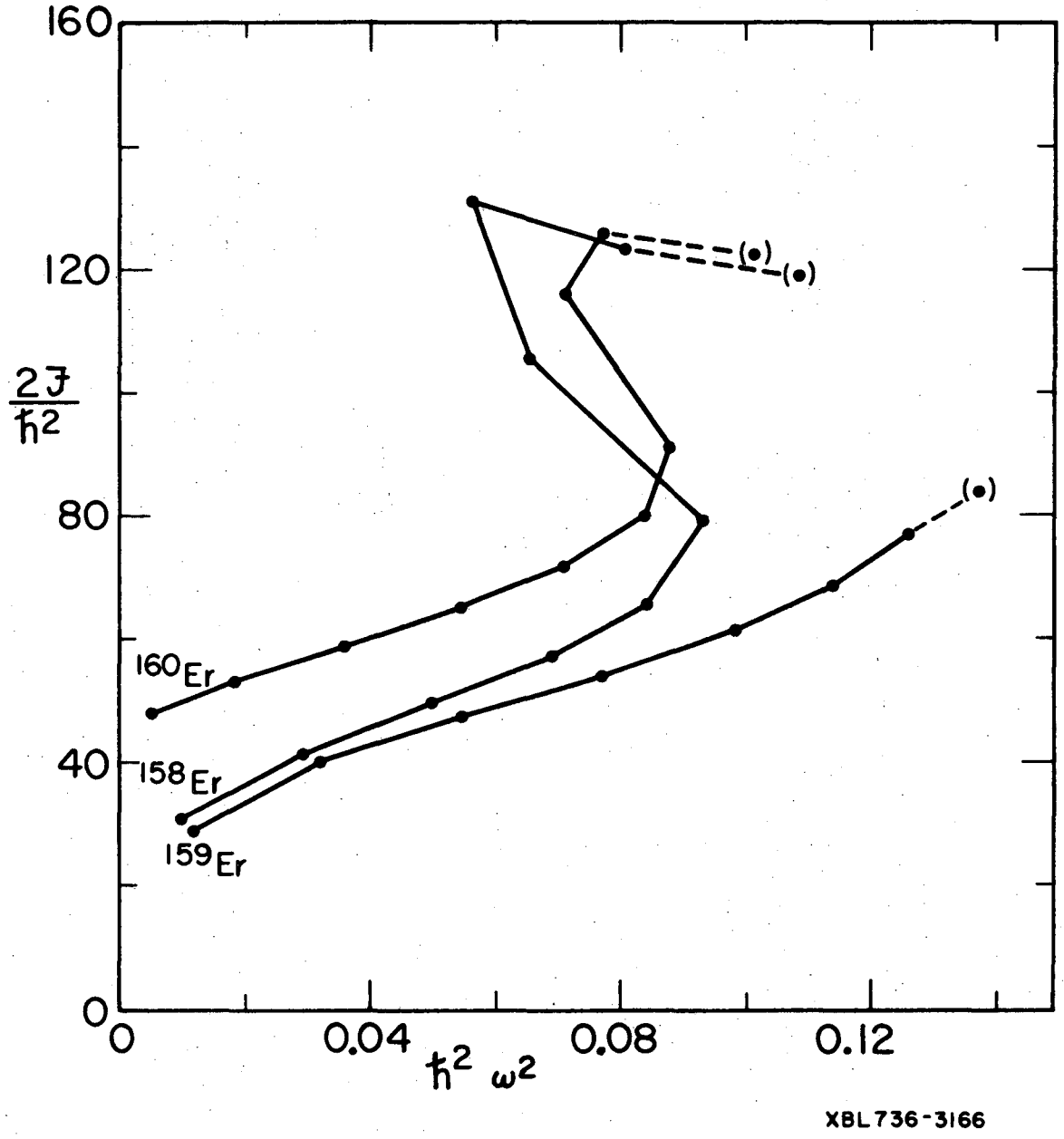
160
120
80
40
0
$\frac{2\mathcal{J}}{\hbar^2}$
0
0.04
0.08
0.12
$\hbar^2\ \omega^2$
^{160}Er
^{158}Er
^{159}Er
(•)
(•)
(•)
XBL736-3166

Fig. 14

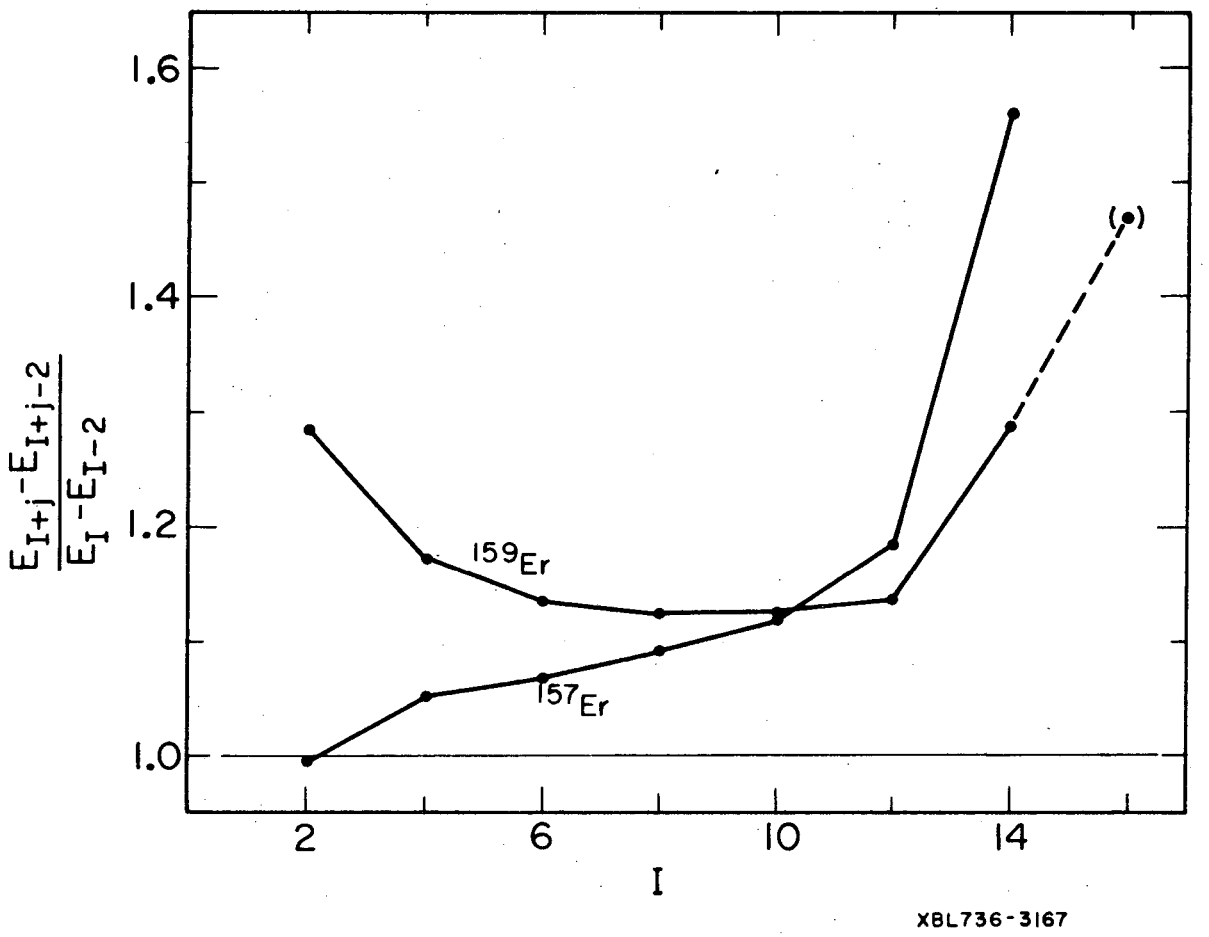
1.6
1.4
1.2
1.0
$\frac{E_{I+j}-E_{I+j-2}}{E_I-E_{I-2}}$
^{159}Er
^{157}Er
(•)
2
6
10
14
I
XBL736-3167

Fig. 15

LEGAL NOTICE

This report was prepared as an account of work sponsored by the United States Government. Neither the United States nor the United States Atomic Energy Commission, nor any of their employees, nor any of their contractors, subcontractors, or their employees, makes any warranty, express or implied, or assumes any legal liability or responsibility for the accuracy, completeness or usefulness of any information, apparatus, product or process disclosed, or represents that its use would not infringe privately owned rights.

TECHNICAL INFORMATION DIVISION
LAWRENCE BERKELEY LABORATORY
UNIVERSITY OF CALIFORNIA
BERKELEY, CALIFORNIA 94720